A Leaky-Wave Antenna Using Periodic Dielectric Perforation for Millimeter-Wave Applications

Priyanka Mondal and Ke Wu

***Abstract*— A periodic leaky-wave antenna is reported in substrate integrated nonradiative dielectric waveguide technology. Periodical change of substrate permittivity along the waveguide channel is used to perturb the propagating LSE_{11} mode. The hosting substrate is perforated following a periodicity to realize the perturbation. Thus, the antenna structure is very easy to implement and suitable for millimeter-wave applications. The antenna scan performance and leakage rate is dependent on the periodicity and size of the perturbation. Guidelines for choice of the parameters along with the condition for radiation of only one beam over the frequency range of interest are discussed. The developed antenna on Alumina substrate shows a good scan performance from −35° to 7° over the frequency range 96 to 108 GHz with a gain better than 10 dBi.**

***Index Terms*— Frequency scanning antenna, periodic leaky-wave antenna (LWA), slow wave, substrate integrated nonradiative dielectric waveguide (SINRD).**

I. Introduction

Leaky-wave antennas (LWAs) are a popular frequency scanning antenna for many decades. There are two types of LWAs depending on the geometry—uniform and periodic [1]. For the uniform LWA, the perturbation is continuous along the length of the guide and for a periodic LWA, periodic perturbation of the guiding structure is required to produce leaky-wave mode radiation. One advantage of periodic LWA is its scanning capability from the backward to the forward quadrant through broadside. Whereas, the scan range of a uniform LWA is limited only to the forward quadrant. Various techniques have been reported in literature to perturb periodically the guiding structure. A series of resonant patch antennas connected by a microstripline is used in [2] for this purpose. In substrate integrated waveguide technology, the distance between two metallic posts is controlled to get considerable leakage [3]. Periodic metallic strip loaded dielectric slab [4], dielectric-inset waveguide [5], and asymmetrically located slots in hybrid planar-planar waveguide technology [6] are some other examples. A periodic LWA is associated with open stopband effect which creates scanning in the broadside direction. But, the effect is controllable by proper choice of perturbation size [6]. However, in all of the above structures, perturbations are in the form of metal patch or slot. Periodic dielectric perturbation can play the same role [7]. But not many are reported. The present structure is based on dielectric perturbation.

Substrate integrated nonradiative dielectric (SINRD) waveguide is a promising candidate for millimeter-wave applications. In this technology, the air region of an NRD guide is replaced by a low-index region having arrays of air holes made on the same substrate. Therefore, the problem of mechanical support and assembling of the planar substrate which arises in case of hybrid planar/NRD scheme can be eliminated [8]. It can support longitudinal-section-electric (LSE) and longitudinal-section-magnetic (LSM) modes. A guideline on the choice of structural parameters for these modes to maximize the bandwidth of operation with minimum transmission loss is given in [9]. In [10], it is shown that SINRD guide can be implemented directly punching on the printed circuit board. As a consequence, it becomes more fabrication friendly in millimeter-wave frequency range.

Manuscript received April 19, 2015; revised May 25, 2016; accepted September 4, 2016. Date of publication October 25, 2016; date of current version December 5, 2016. This work was supported by the Fonds Québécois de la Recherche sur la Nature et les Technologies Postdoctoral Fellowship, Quebec, Canada.

P. Mondal was with the Poly-Grames Research Center, École Polytechnique de Montréal, Montréal, QC H3T 1J4, Canada. She is now with the National Institute of Technology Patna, Patna 800005, India (e-mail: pmondal@ieee.org).

K. Wu is with the Poly-Grames Research Center, École Polytechnique de Montréal, Montréal, QC H3T 1J4, Canada (e-mail: ke.wu@polymtl.ca).

Color versions of one or more of the figures in this communication are available online at http://ieeexplore.ieee.org.

Digital Object Identifier 10.1109/TAP.2016.2621032

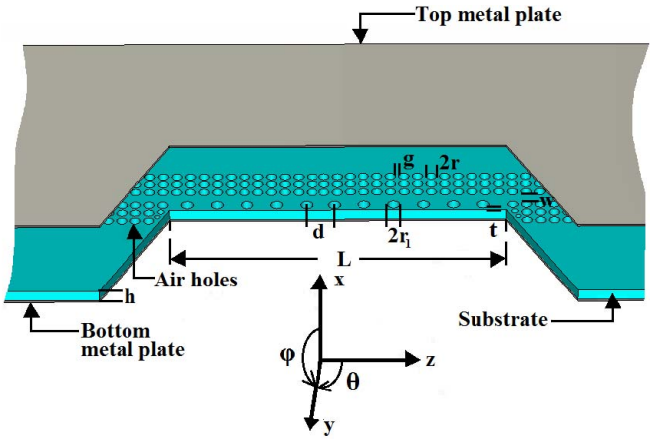

Fig. 1. Configuration of the periodic LWA. Top metal plate is shifted upward to show the structure.

The fundamental LSE (LSE_{11}) and LSM (LSM_{11}) modes are degenerate modes and they are orthogonal in space. But, coupling between the modes occurs at the bends and discontinuities which necessitate mode suppressors. In [11], it is shown that LSE_{11} mode can lead to single mode of operation by proper selection of structural parameters. Moreover, it can provide lower propagation loss than that of LSM_{11} mode [12], under certain conditions. Thus, it can be a preferable mode of propagation. Being a perforated structure, a SINRD waveguide gives rise to interesting features [13]. Here, a simple procedure is presented to design a periodic LWA in this technology. The periodic perforation along its channel is curbed to radiate over a frequency band of interest.

II. Antenna Structure and Working Principle

Proposed LWA is shown in Fig. 1. It consists of unperturbed and perturbed waveguide sections. The unperturbed sections are to connect to the source and load. There are three rows of air holes with square lattice configuration on both sides of the channel. In the perturbed section, one side of the channel is replaced by a single row of sparsely distributed air holes (periodicity $= d$) as shown in the figure.

The dispersion curve of a SINRD waveguide without any perturbation for LSE_{11} mode is shown in Fig. 2. The Eigenmode solver of CST Microwave Studio is used to compute the phase constant and a 25 mil thick Alumina substrate of dielectric constant 9.9 and loss tangent 0.0001 (at 1 MHz) is considered for computations. Structural dimensions are as follows: $w = 25$ mil, $r = 12$ mil, and $g = 6$ mil. Here, it is chosen $r \geq 0.4p$ where $p = 2r+g$. With this choice, cutoff frequency of parallel plate mode in the low index region of SINRD waveguide which primarily limits the transmission bandwidth [9] is pushed to a substantial higher frequency and hence the maximum usable frequency. The maximum usable frequency of the waveguide corresponding to the present hole profile is 106.5 GHz.

The dispersion curve shows that it consists of a fast as well as a slow wave part. If an asymmetry is introduced to the waveguide by

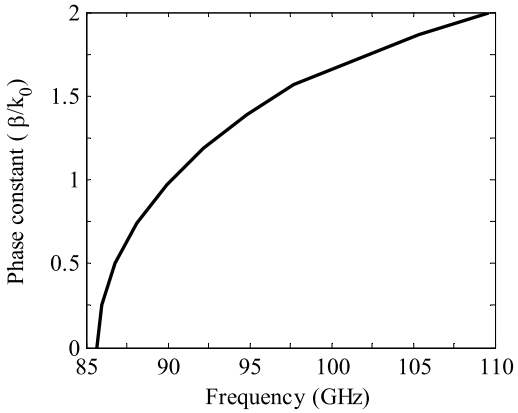

Fig. 2. Phase constant of SINRD waveguide for LSE_{11} mode.

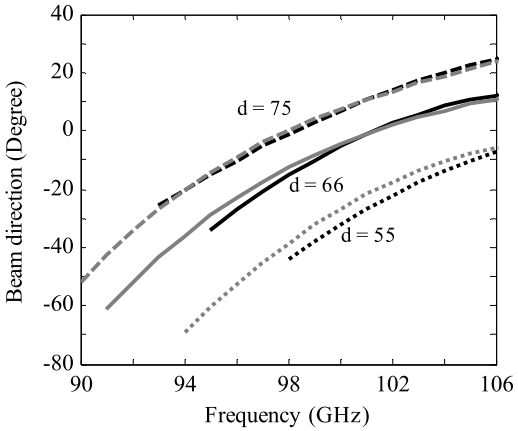

Fig. 3. Calculated (gray) and simulated (black) beam directions for different periodicity. The dimensions are in mil.

replacing three rows of air holes with a single one ($d = p$) and the metal plates are truncated as shown in Fig. 1, leaky-wave radiation occurs. But it is in the fast-wave frequency band as is reported in [14]. The fast-wave region of the present waveguide ends at 90.2 GHz (see Fig. 2). Now, if the air holes in the perturbed section is distributed sparsely ($d > p$) again radiation occurs but it is in the slow wave frequency band of the propagating mode. The sparsely distributed air holes is modulating the substrate permittivity which in turn is acting as the disturbance to the propagating mode. Therefore, one of the constituent space harmonics tends to become a fast-wave depending on the frequency although the propagating mode is a slow wave.

The direction of maximum radiation for a particular periodicity can be computed by [1]

$$\mathrm{Sin}\theta_m = \frac{\beta}{k_0} + \frac{n\lambda_0}{d} \tag{1}$$

where θ_m is the direction of maximum radiation from broadside, β is the phase constant of the dominant mode of propagation of the unperturbed waveguide, i.e., here for LSE_{11} mode, n is the space harmonic and λ_0 and k_0 are the free space wavelength and wavenumber, respectively. Beam directions for different periodicity obtained by putting $n = -1$ in (2) and full-wave simulations are plotted in Fig. 3. The Transient solver of CST Microwave Studio with $r_1 = 12$ mil, $L = 1080$ mil, and $t = 8$ mil is used for the full-wave simulations. Although (2) assumes infinite periodic structure, Fig. 3 shows that it holds good even for the finite structure. It can be noted from (2) that only the negative space harmonics can produce fast-wave since $(\beta/(k_0))$ is greater than one in the slow wave frequency band. The space harmonic which at first become fast is $n = -1$. With the increase of frequency, the next negative space

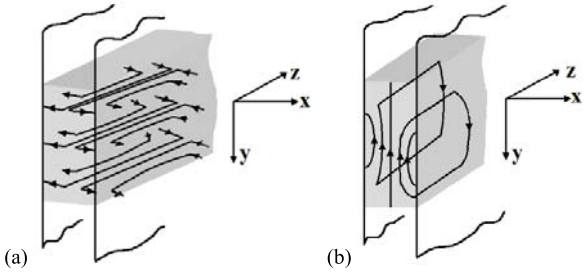

Fig. 4. E-field pattern of (a) LSE_{11} and (b) LSM_{11} modes.

harmonic ($n = -2$) tends to be a fast-wave and may peep through the back-fire direction. Thus, the choice of periodicity to ensure a radiated beam and only one beam in the frequency band of interest is given by

$$\frac{1}{1+\frac{\beta}{k_0}} < \frac{d}{\lambda_0} < \frac{2}{1+\frac{\beta}{k_0}}. \tag{2}$$

It is to note that the frequency band of operation having only one radiating beam should be chosen below the maximum usable frequency of the SINRD waveguide, e.g., in the present case it is 106.5 GHz.

Electric field distributions of LSE_{11} and LSM_{11} modes are shown in Fig. 4. LSE_{11} mode being an LSE mode is perturbed by the proposed arrangement rather than its LSM_{11} counterpart. The present antenna structure does not involve any metallic patch which requires accurate placement and precise dimensions in millimeter-wave frequencies. Thus, it is easy to fabricate and can be made mechanically stable even in upper millimeter-wave frequencies.

III. Effects of Perturbation on Radiation Characteristics

This section is to discuss about the effect of periodicity and perturbation size on the radiation characteristics such as the direction of maximum radiation and leakage constant. In Fig. 3, the full-wave simulated beam directions show that there is no leaky-wave mode at the lower frequencies although a wider range of beam direction is predicted by computation. Therefore, the scan range is reduced considerably in the backward quadrant. So, for proper excitation of the leaky-wave mode in the lower end, another series of smaller air holes is used in between the primary air holes. The modified structure is shown in Fig. 5. Periodicity of the secondary air holes is kept the same as d. In the present study, r_2 is kept fixed as 5 mil. Other structural parameters remain the same as mentioned in the previous section. The leakage constant due to radiation is computed by [1]

$$P_{\mathrm{rad}} = 1 - \frac{P(L)}{P(0)} \tag{3a}$$

$$\text{and } P(L) = P(0)e^{-2\alpha L} \tag{3b}$$

where P_{rad} is the radiated power through the radiating aperture of length L and $P(0)$ and $P(L)$ are the powers at the input and output ends of the aperture, respectively. To compute leakage due to radiation only, perfect electric conductors and lossless substrates are considered in the full-wave simulations. The radiated power is obtained by subtracting the reflected and transmitted power from the total power.

A. Periodicity of Perturbation

The effect of periodicity d on the beam direction and leakage constant are shown in Fig. 6(a) and (b), respectively. Here, the primary air hole size is kept fixed at $r_1 = 12$ mil. It is to note from Figs. 3 and 6(a) that introduction of the secondary holes improves the scan performance in the lower frequency end considerably. For an

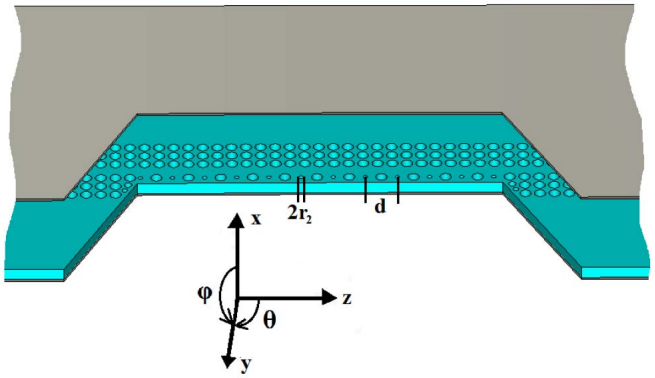

Fig. 5. Configuration of the modified LWA with secondary air holes.

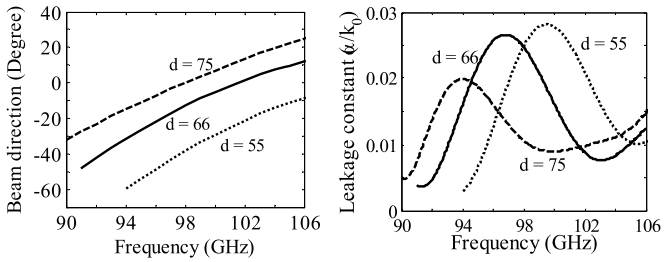

Fig. 6. (a) Direction of maximum radiation. (b) Leakage constant for different periodicities. d is in mil.

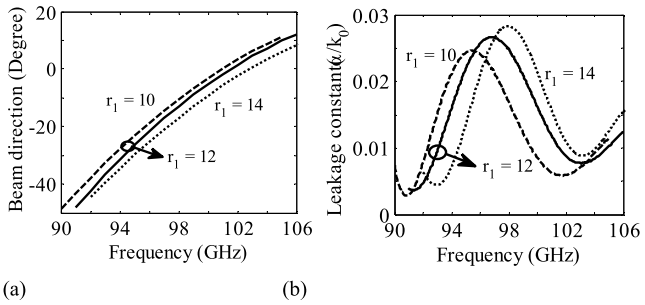

Fig. 7. (a) Direction of maximum radiation. (b) Leakage constant for different perforation sizes. d is in mil.

example, for $d = 66$ mil, the beam scanning starts at $-34°$ at 95 GHz in Fig. 3 whereas for the modified structure it appears at $-48°$ at 91 GHz. Now, periodicity has a significant effect on antenna scan performance. It is to choose periodicity in the lower end given by (2) for scanning in the backward quadrant. But it becomes difficult to scan through broadside as can be noted from $d = 55$ mil. Similarly, longer periodicity leads positive scan angle.

For a particular periodicity, leakage rate attains the maximum at a frequency and decreases on both sides [see Fig. 6(b)]. In addition, the leaky-wave mode radiation shifts toward higher frequency for smaller periodicity as is evident from (2). Thus, the frequency corresponding to maximum radiation also shifts toward high frequency for smaller periodicity. The leakage rate again starts to increase around 106 GHz. This is because of the onset of parallel plate mode. It also contributes in the leakage.

B. Size of Perturbation

Similarly, the effect of perturbation size, i.e., diameter of air holes, is plotted in Fig. 7. Here, r_1 is varied from 10 to 14 mil and the periodicity is kept fixed at $d = 66$ mil. No significant change in scan performance [Fig. 6(a)] is observed except a slight increase in

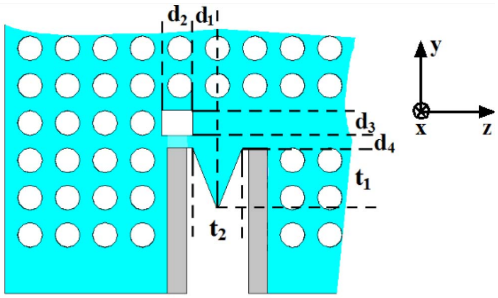

Fig. 8. Top view of the rectangular waveguide to SINRD waveguide transition. Top metal plate is removed.

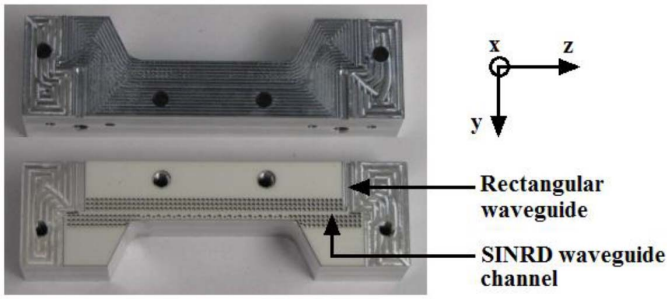

Fig. 9. Photograph of the fabricated antenna.

the leakage constant with the increase of perturbation size. It can be interpreted as the bigger air hole produces electromagnetically larger disturbance to the propagating mode and hence more leakage. As a consequence, the effect can be utilized for amplitude tapering to control sidelobe level. The truncation distance t between the edge of the air hole perturbation and the metal plate as shown in Fig. 1 has significant effect on the leakage constant as is mentioned in [14]. It increases with decreasing t due to the exponential decay of the field in lateral direction. In this communication, t is kept as 8 mil. An even smaller value of t leads to substrate fragility.

IV. Fabrication and Experimental Verification

For an example, an antenna is designed and fabricated on a 25 mil thick Alumina substrate using computer controlled laser guided drilling machine. The metal plates are made of Aluminum. The length of the radiating aperture is $L = 1080$ mil $\sim 9\lambda_0$ at 97 GHz. For $r_1 = 12$ mil, leakage rate is the highest around 97 GHz. Perturbation size is kept uniform throughout the aperture. Other structural parameters are $w = 25$ mil, $r = 12$ mil, $g = 6$ mil, and $r_2 = 5$ mil. The measurement setup is based on rectangular waveguide. So, the transition scheme of [11] from rectangular waveguide to SINRD waveguide is adopted for excitation of LSE_{11} mode. The structure of the transition is shown in Fig. 8. The optimized structural parameters for the present band of interest are $t_1 = 60$ mil, $t_2 = 25$ mil, $d_1 = 5$ mil, $d_2 = 27$ mil, $d_3 = 13$ mil, and $d_4 = 6$ mil. A photograph of the fabricated antenna is shown in Fig. 9. An Anritsu 3739C network analyzer with the WR10 extension is used for the scattering parameters measurements. The radiation characteristics are measured in a compact range anechoic chamber.

Measured and simulated S-parameters together with the transition are shown in Fig. 10. Permittivity and loss tangent of Alumina substrate at 100 GHz are reported as 9.6 and 0.0006, respectively [15]. These values are considered in simulations together with the Aluminum metal plates. Moreover, due to laser drilling air holes are oversized by 2 mil. So, the considered hole sizes for the simulations in Fig. 10 are $r = 13$ mil, $r_1 = 13$ mil, and $r_2 = 6$ mil.

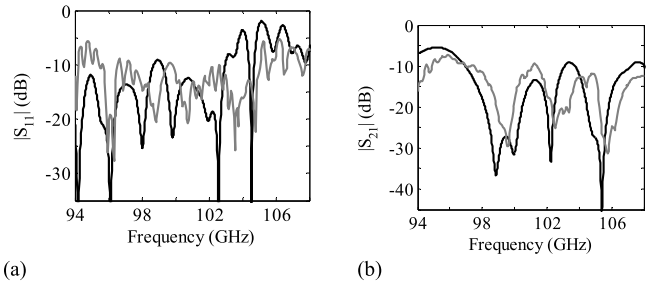

Fig. 10. Measured (gray) and simulated (black) (a) S_{11} and (b) S_{21} of the fabricated antenna.

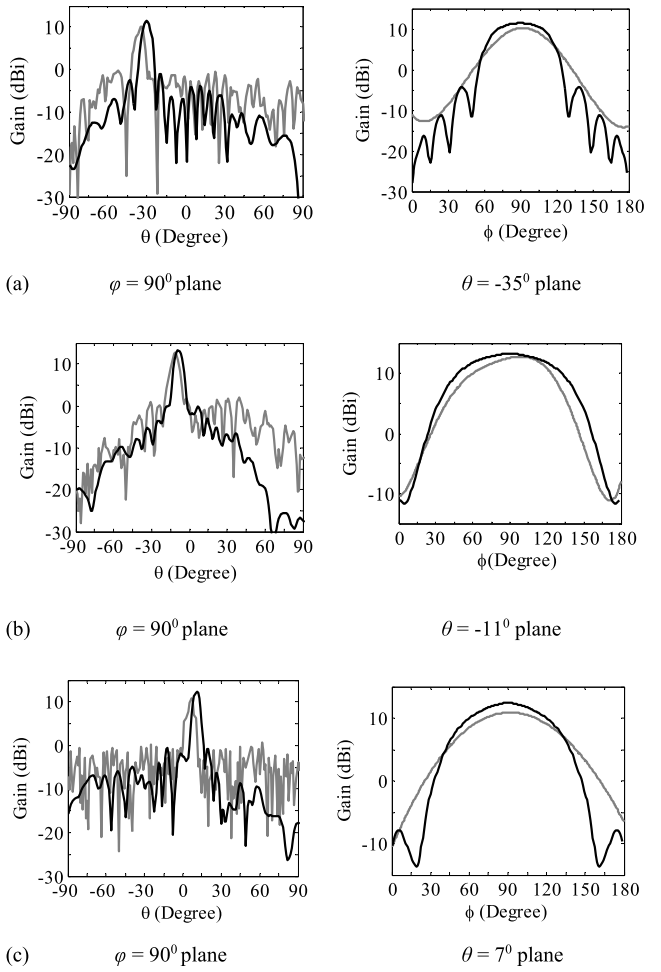

Fig. 11. Measured (gray) and simulated (black) radiation patterns of the antenna at (a) 96, (b) 102, and (c) 108 GHz.

Measured and simulated radiation patters in $\varphi = 90°$ plane and the respective θ planes are shown in Fig. 11 at three different frequencies. The antenna has a very good scan capability from $-35°$ to $7°$ over the frequency range 96–108 GHz. Measured antenna gain is 12.7 dBi at 102 GHz and on either side, it is better than 10 dBi. One reason for gain variation is the performance of rectangular waveguide to SINRD waveguide transition. The transition has the lowest insertion loss in the mid band frequency. Measured sidelobe level over the frequency band is better than -10.5 dB. A higher reflection is observed around the broadside radiation frequency ($\sim$105 GHz). This is due to the open stopband effect. Simulations show that cross-polarization level is below -30 dB in the direction of maximum radiation.

V. Conclusion

A periodic LWA is proposed by introducing air holes having periodicity determined by the wavelength along the channel of SINRD waveguide. The first negative space harmonic becomes a fast-wave due to this arrangement and radiation occurs even if the propagating mode is a slow wave in nature. Precautions would have to take to choose the hole profile of the unperturbed SINRD waveguide so that the desired frequency band is within the maximum usable frequency of the guide. Parametric study shows that closer spacing of the perturbing air holes leads to negative angle scanning whereas for the positive scan angle it is required to push the air holes farther. Moreover, for a particular periodicity, leakage rate is dependent on the diameter of perforation. It can be exploited to control sidelobe level.

Acknowledgment

The authors would like to thank S. Dube and M. Thibault of Poly-Grames Research Center for fabrication and measurements, respectively.

References

[1] A. A. Oliner and R. C. Johnson, "Leaky-wave antennas," in *Antenna Engineering Handbook*, 3rd ed. New York, NY, USA: McGraw-Hill, 1993, ch. 10.

[2] A. Derneryd, "Linearly polarized microstrip antennas," *IEEE Trans. Antennas Propag.*, vol. 24, no. 6, pp. 846–851, Nov. 1976.

[3] F. Xu, K. Wu, and X. Zhang, "Periodic leaky-wave antenna for millimeter wave applications based on substrate integrated waveguide," *IEEE Trans. Antennas Propag.*, vol. 58, no. 2, pp. 340–347, Feb. 2010.

[4] J. Jacobsen, "Analytical, numerical, and experimental investigation of guided waves on a periodically strip-loaded dielectric slab," *IEEE Trans. Antennas Propag.*, vol. 18, no. 3, pp. 379–388, May 1970.

[5] M. Guglielmi and G. Boccalone, "A novel theory for dielectric-inset waveguide leaky-wave antennas," *IEEE Trans. Antennas Propag.*, vol. 39, no. 4, pp. 497–504, Apr. 1991.

[6] J. L. Gomez-Tornero, F. D. Quesada-Pereira, and A. Alvarez-Melcon, "Analysis and design of periodic leaky-wave antennas for the millimeter waveband in hybrid waveguide-planar technology," *IEEE Trans. Antennas Propag.*, vol. 53, no. 9, pp. 2834–2842, Sep. 2005.

[7] F. K. Schwering and S.-T. Peng, "Design of dielectric grating antennas for millimeter-wave applications," *IEEE Trans. Microw. Theory Techn.*, vol. 31, no. 2, pp. 199–209, Feb. 1983.

[8] Y. Cassivi and K. Wu, "Substrate integrated NRD (SINRD) guide in high dielectric constant substrate for millimetre wave circuits and systems," in *IEEE MTT-S Int. Microw. Symp. Dig.*, vol. 3. Jun. 2004, pp. 1639–1642.

[9] P. Mondal and K. Wu, "Optimum structural parameters of substrate integrated nonradiative dielectric waveguide for millimeter-wave applications," in *Proc. IEEE Appl. Electromagn. Conf.*, Dec. 2015, pp. 146–147.

[10] F. Xu and K. Wu, "Substrate integrated nonradiative dielectric waveguide structures directly fabricated on printed circuit boards and metallized dielectric layers," *IEEE Trans. Microw. Theory Techn.*, vol. 59, no. 12, pp. 3076–3086, Dec. 2011.

[11] P. Mondal and K. Wu, "Single mode operation of substrate integrated non-radiative dielectric waveguide and an excitation scheme of LSE_{11} mode," *IEEE Microw. Wireless Compon. Lett.*, vol. 23, no. 8, pp. 418–420, Aug. 2013.

[12] J. Dallaire and K. Wu, "Complete characterization of transmission losses in generalized nonradiative dielectric (NRD) waveguide," *IEEE Trans. Microw. Theory Techn.*, vol. 48, no. 1, pp. 121–125, Jan. 2000.

[13] P. Mondal and K. Wu, "A leaky-wave antenna in substrate integrated non-radiative dielectric (SINRD) waveguide with controllable scanning rate," *IEEE Trans. Antennas Propag.*, vol. 61, no. 4, pp. 2294–2297, Apr. 2013.

[14] A. Sanchez and A. A. Oliner, "A new leaky waveguide for millimeter waves using nonradiative dielectric (NRD) waveguide—Part I: Accurate theory," *IEEE Trans. Microw. Theory Techn.*, vol. 35, no. 8, pp. 737–747, Aug. 1987.

[15] M. N. Afsar, "Dielectric measurements of millimeter-wave materials," *IEEE Trans. Microw. Theory Techn.*, vol. 32, no. 12, pp. 1598–1609, Dec. 1984.